JOURNAL OF PROPULSION AND POWER
Vol. 25, No. 1, January–February 2009

# Time Delay Analysis of Turbofan Engine Direct and Indirect Combustion Noise Sources

Jeffrey Hilton Miles*
*NASA John H. Glenn Research Center at Lewis Field, Cleveland, Ohio 44135*

DOI: 10.2514/1.38030

**The core noise components of a dual-spool, turbofan engine were separated by the use of a coherence function. A source location technique based on adjusting the time delay between the combustor pressure sensor signal and the far-field microphone signal to maximize the coherence and remove as much variation of the phase angle with frequency as possible was used. It was discovered that, for the 130 deg microphone, a 90.027 ms time shift worked best for the frequency band from 0 to 200 Hz, whereas an 86.975 ms time shift worked best for the frequency band from 200 to 400 Hz. Hence, the 0–200 Hz band signal took more time than the 200–400 Hz band signal to travel the same distance. This suggests the 0–200 Hz coherent cross-spectral density band is partly due to indirect combustion noise attributed to entropy fluctuations, which travel at the flow velocity, interacting with the turbine. The signal in the 200–400 Hz frequency band is attributed mostly to direct combustion noise. Results are presented herein for engine power settings of 48, 54, and 60% of the maximum power setting.**

## Nomenclature

| | | |
|---|---|---|
| $B_e$ | = | resolution bandwidth, Hz, $B_e = 1/T_d = r/NP =$ 16 Hz |
| $D$ | = | propagation time delay or lag, s |
| $f$ | = | frequency, Hz |
| $f_c$ | = | upper frequency limit, $f_c = 1/2\Delta t = r/2$, Hz (32,768 Hz) |
| $G_{xx}(f)$ | = | auto power spectral density function defined for nonnegative frequencies only (one-sided) |
| $G_{xy}(f)$ | = | cross-power spectral density function defined for nonnegative frequencies only (one-sided) |
| $H(f)$ | = | transfer function frequency response |
| $h(\tau)$ | = | weighting function or unit impulse response function |
| $L_y$ | = | number of frequencies, $f_c/\Delta f = N/2$ (2048) |
| $N$ | = | segment length, number of data points per segment (4096) |
| $n_s$ | = | number of disjoint (independent) data segments/ blocks, $n_s = B_e T_{\text{total}} = 1120$ |
| $P$ | = | $P$-percent confidence interval |
| $r$ | = | sample rate, samples/s (65,536) |
| $s_c(t)$ | = | combustor input signal |
| $s_F(t)$ | = | far-field output signal |
| $T_d(i)$ | = | record length of segment $i$, $N/r$, 0.0625 s |
| $T_{\text{total}}$ | = | total record length, s ($\approx$70 s) |
| $W_{s_F s_F}(f)$ | = | coherent output power spectral function |
| $\gamma^2_{nn}(f)$ | = | magnitude squared noise coherence, 0.00267 |
| $\gamma^2_{xy}(f)$ | = | magnitude squared coherence function |
| $\Delta f$ | = | frequency step, $1/T_d$, Hz (16 Hz) |
| $\Delta t$ | = | sampling interval, $1/r$ (1/65 536) s |
| $\theta_{xy}(f)$ | = | cross-spectrum phase angle |

*Subscripts*

| | | |
|---|---|---|
| $i$ | = | running segment index |
| $K(t)$ | = | combustor pressure transducer sensor signal |
| $M(t)$ | = | far-field microphone signal |
| $n(t)$ | = | signal noise |
| $x(t)$ | = | signal $x$ |
| $y(t)$ | = | signal $y$ |

## I. Introduction

TURBOFAN engine noise test programs are conducted to create noise reduction technology and to identify dominant noise sources. Core noise is of interest because it may become a significant contributor to the overall turbofan engine noise when the fan and jet noise are reduced because of forward velocity effects (particularly during approach). In addition, future advances in fan and jet noise reduction technologies may cause core noise to be a more significant contributor to the overall turbofan engine noise.

One source of turbofan engine combustion noise is attributed to the unsteady pressures produced by the unsteady combustion process that propagate through the turbine to the far field. This is known as a "direct" combustion noise mechanism. The relation between heat release and pressure waves was studied by Chu (1955) [1]. Strahle (1971) [2] developed a framework that explained past experimental studies of direct combustion-generated noise from flames using an approach similar to the one Lighthill (1952, 1954) [3,4] used in his studies of aerodynamic noise. Further developments in scaling laws were derived by Strahle (1972) [5] and Strahle and Shivashankara (1975) [6] involving the first Eulerian time derivative of the chemical reaction rate integrated over the reacting volume. A review of current theories of scaling laws is given by Strahle (1975) [7]. The study of combustion-generated noise from turbulent flames is a continuing area of research. For example, the spectral characteristics of premixed flame noise has been studied by Rajaram and Lieuwen (2003) [8] and Rajaram et al. (2006) [9], and large-eddy simulation computations to predict combustion-generated noise in nonpremixed turbulent jet flames have been conducted by Ihme et al. (2006) [10]. Thermoacoustic sources and instabilities are discussed by Dowling (1992) [11].

Another source of turbofan engine combustion noise is known as the "indirect" mechanism in which the noise is generated in the turbine by the interaction of entropy fluctuations ("hot spots"), which also originate from the unsteady combustion process. This indirect source was studied by Pickett (1975) [12], Cumpsty and Marble (1977) [13,14], Cumpsty (1979) [15], and Gliebe et al. (2000) [16]. The indirect mechanism also functions when an entropy fluctuation interacts with an area change as shown by Cuadra (1967) [17] or a

Presented as Paper 50 at the 46th AIAA Aerospace Sciences Meeting and Exhibit, Reno, NV, 7–10 January 2008; received 11 April 2008; revision received 21 September 2008; accepted for publication 25 September 2008. 

*Aerospace Engineer, Acoustics Branch, 21000 Brookpark Road. AIAA Member.

nonuniform flow as shown by Goldstein (1979) [18], and when an entropy or density nonuniformity is convected through a nozzle as shown by Williams and Howe (1975) [19] and Marble and Candel (1977) [20]. Further discussions of indirect and direct combustion noise can be found in the review article by Strahle (1977, 1978) [21,22].

A program to develop and evaluate improved methods for predicting indirect and direct combustion noise was conducted by Mathews et al. (1977) [23]. However, during the study, comparison of predictions with full-scale engine data indicated that direct combustion noise is the dominant source for the engines investigated. As a consequence, this report and a summary by Mathews and Rekos (1977) [24] discuss only direct combustion noise.

Strahle et al. (1977) [25] investigated direct combustion noise from an isolated combustor can and discuss the problem of the mixture of "pseudosound" and sound in a combustor. The coherent combustion noise is discussed and the presence of incoherent noise is noted. Coherence between pressure measurements in the can combustor and far-field microphones are discussed and analyzed using a combustion acoustic model. Muthukrishnan et al. (1978) [26] discuss tests using a nozzle attached to the combustor can. The importance of direct noise and indirect noise (noise from hot spots passing through area changes and gradients) is discussed. Without the nozzle, when no pressure drop occurred downstream of the combustor, the far-field noise was due to a direct combustion noise mechanism. When the flow was accelerated by the nozzle, the indirect combustion noise mechanism appeared dominant.

Miles et al. (1983) [27] measured the cross spectra between temperature and pressure in a constant area duct downstream of a combustor and showed that the entropy fluctuations (hot spots) moved with the flow speed. Schemel et al. (2004) [28] experimentally and numerically studied entropy noise generated by hot spots (from a combustor) passing through a nozzle. Richter et al. (2005) [29] studied the application of computational aeroacoustic methods to indirect combustion noise generated by hot spots passing through a nozzle. Bake et al. (2005, 2007) [30,31] verified that the entropy fluctuations (hot spots) moved with the flow speed. The first paper studied experimentally and numerically indirect combustion noise generated by hot spots (from a combustor) passing through a nozzle. The second paper studied experimentally indirect combustion noise generated by hot spots (created by electrical heating) passing through a nozzle.

The net travel time of the indirect combustion noise signal from the combustor to the far field is increased because the travel velocity of the hot spots to the turbine and in the turbine is the flow velocity. This flow velocity is a small fraction of the speed of sound. Miles et al. (1983) [27] has shown the pressure and entropy should be in phase in the combustor. Consequently, one might expect that the pressure signal from an indirect combustion noise source would be delayed relative to a pressure signal from a direct combustion noise source because an indirect combustion noise signal does not travel with the speed of an acoustic wave until it interacts with the turbine. It is shown herein that the cross spectra is a tool that provides a way to measure this time delay. Using this tool, direct and indirect coherent combustion noise can be separated.

## II. Turbofan Engine Coherence Function Measurements

The data analyzed are from a Honeywell TECH977 dual-spool, turbofan engine. The particular test data set analyzed herein consisted of signals from one pressure transducer in the combustor, two pressure transducers in the low-pressure turbine exit, two pressure transducers in the bypass duct, and eight far-field microphones. However, the signals from the combustor pressure transducer and the signals from the three downstream rear-quadrant far-field microphones at 110, 130, 160 deg are the only ones used in the present study.

The dual-spool turbofan engine has a direct drive, wide chord fan connected by a long shaft (designated as N1) to the low-pressure turbine spool and a high-pressure compressor connected by a concentric short shaft (designated as N2) to the turbine high-pressure spool. The combustor located between the compressor and the turbine has a straight through annular shape with 16 fuel nozzles and 2 ignitors. The high-pressure hot flow from the combustor turns the turbine spools which, due to the connecting shafts, turns the fan and the compressor. The pressure transducer in the combustor replaces one of the ignitors and is identified herein as CIP1. The dependent source separation technique used herein to separate direct combustion noise and indirect combustion noise is feasible due to the availability of data from the CIP1 transducer location.

The results presented herein (see Sec. III) for the 130 deg microphone are extracted from a discussion of coherence function calculations of the turbofan engine coherent combustion noise component [Eq. (8)] made using far-field microphones and the combustor pressure transducer presented by Miles (2008) [32]. Test results at 10, 30, 50, 70, 90, 110, 130, and 160 deg are presented using the alignment time delay for the indirect combustion noise, showing coherent core noise directivity in terms of the coherent output power of the combustion noise (also known as the coherent combustion noise spectrum) in part d of Figs. 6–29 of [32]. The coherent combustion noise spectrum, coherence function, and cross-spectrum phase-angle plots shown in Figs. 6–29 of [32] are based on the time delays in Table 3 of [32], which are the indirect core noise time delays. Examination of these plots indicates that the best way to demonstrate the results presented herein is to use the 130 deg microphone data. Acoustic data from the same TECH977 engine test program are discussed by Alonso et al. (2008) [33], Mendoza et al. (2008) [34], Weir and Mendoza (2008) [35], Schuster (2008) [36], Royalty and Schuster (2008) [37], and Dougherty and Mendoza (2008) [38]. These papers indicate the scope of the test program.

Similar coherence function analysis was used starting 30 years ago to evaluate core noise from several engines. The following examples come to mind: an AVCO Lycoming YF-102 by Karchmer and Reshotko (1976) [39], Karchmer (1977) [40], Reshotko et al. (1977) [41], and Krejsa (1987) [42]; an APU by Shivashankara (1978) [43]; the General Electric CF6-50 by Doyle and Moore (1980) [44]; the Pratt and Whitney JT15D by Reshotko and Karchmer (1980) [45]; and the Pratt and Whitney JT9D by Shivashankara (1983) [46]. In the same time period, the coherence function between a combustor pressure sensor and a far-field microphone was measured for a gas turbine combustor using a single fuel spray nozzle assembly taken from a Boeing 502-7D gas turbine unit by Strahle et al. (1977) [25] and Muthukrishnan et al. (1978) [47] in studies of turbofan engine core noise.

Core noise of a Rolls-Royce BR700 aeroengine has also been studied with the aid of a phased linear array of microphones by Siller et al. (2001) [48] and a combustor pressure sensor. Coherence between the combustor pressure sensor and a phased-array signal was obtained and the coherent array output power spectrum was measured.

Recently, coherence function analysis techniques were used to evaluate core noise from a Pratt and Whitney PW4098 by Miles (2006) [49]. The data evaluated were acquired from a test conducted as part of the NASA Engine Validation of Noise Reduction Concepts program in 2001. In the time interval between 1980 and 2000, turbofan engine designs have changed with newer engines being based on new materials and a longer history of experience in turbofan manufacturing, design, analysis, and optimization. In evaluating the PW4098 core noise data, it was found that one consequence of these design changes is that the coherent part of the core noise signal has decreased [49]. To evaluate small coherence function values, a new diagnostic tool using aligned and unaligned coherence functions was developed. This tool, which is explained by Miles [49], also needs to be applied to signals acquired in this test program because the core noise coherence values are small.

## III. Coherent Output Power Spectrum

In the past, methods have been developed using spectrum analysis techniques to characterize acoustic signals from different sources

mixed with noise. Bendat and Piersol (1966, 1971, 1980) [50–52] discuss these methods. Among the methods discussed is one using coherent output power spectra [Eq. (8)] for noise source identification. The application of this technique that is of interest is the use of coherent output power spectra to separate and identify correlated combustion noise in far-field measurements of turbofan engine noise. Karchmer (1977) [40] and Karchmer et al. (1977) [53] use the coherence function calculated from internal microphone measurements of fluctuating pressures in the combustor and far-field acoustic pressures to determine the correlated combustion noise of a YF102 turbofan engine at far-field locations by calculating the coherent output power spectrum. A typical result showed that the coherence [Eq. (6)] measured between the combustor pressure and the 120 deg far-field acoustic pressure had a roughly Gaussian-shaped distribution in the range of 0–200 Hz with a peak near 125 Hz and a maximum value at 30% fan speed of 0.38 and, at 43% fan speed, a maximum value of 0.5 ([40], Figs. 39, 48). The corresponding combustion coherence output power spectrum for the 43% fan speed case has a peak near 125 Hz and a generally domelike shape. The peak is about $20\log(0.5) = -6.02$ dB below the peak of the far-field spectrum at 120 Hz. The dome edges are 20 dB down at 40 and 200 Hz.

The basic formulation for the coherent output power spectrum is presented by Bendat and Piersol (1980) [52]. We assume that the far-field output signal $s_F$ is the output of a constant parameter linear system with weighting function $h(\tau)$ and frequency response $H(f)$. The output of the system is given by the convolution integral of the combustor input signal $s_c(t)$:

$$s_F(t) = \int_0^\infty h(\tau) s_c(t-\tau)\,\mathrm{d}\tau \tag{1}$$

Then, the far-field combustion noise spectrum $G_{s_F s_F}(f)$ and the combustion noise cross spectrum between the far-field signal and the combustor pressure sensor signal $G_{s_F s_c}(f)$ are related to the combustor pressure sensor signal as follows:

$$G_{s_F s_F}(f) = |H(f)|^2 G_{s_c s_c}(f) \tag{2}$$

$$G_{s_F s_c}(f) = H(f) G_{s_c s_c}(f) \tag{3}$$

Here, the cross-power spectrum between the combustor pressure sensor signal $x(t)$ and the far-field microphone signal $y(t)$ is $\hat{G}_{xy}(f)$, and the corresponding combustor pressure sensor power spectra and far-field spectra are $\hat{G}_{xx}(f)$ and $\hat{G}_{yy}(f)$.

We have

$$\hat{G}_{xx}(f) = \hat{G}_{s_c s_c}(f) + \hat{G}_{n_1 n_1}(f) \tag{4}$$

$$\hat{G}_{yy}(f) = \hat{G}_{s_F s_F}(f) + \hat{G}_{n_2 n_2}(f) \tag{5}$$

where $\hat{G}_{n_1 n_1}(f)$ and $\hat{G}_{n_2 n_2}(f)$ represent uncorrelated noise spectra.

These are obtained by averaging many ($\approx$2000) successive, directly calculated, power spectral densities using a 70 s total observation time, a sampling rate of $2^{16} = 65,536$ samples/s, and a 50% overlap in the spectrum calculations. In practice, only estimates, $\hat{G}_{xy}(f)$ of $G_{xy}(f)$, $\hat{G}_{xx}(f)$ of $G_{xx}(f)$, and $\hat{G}_{yy}(f)$ of $G_{yy}(f)$, can be obtained due to the finite observation interval, and the ^ notation will be dropped.

The combustion noise reaching a microphone will be estimated using the magnitude squared coherence function $\gamma^2_{xy}(f)$, where

$$\gamma^2_{xy}(f) = \frac{|G_{xy}(f)|^2}{G_{xx}(f) G_{yy}(f)} \tag{6}$$

Then,

$$|G_{xy}(f)|^2 = |G_{s_F s_c}(f)|^2 = |H(f)|^2 G^2_{s_c s_c}(f) = G_{s_F s_F}(f) G_{s_c s_c}(f) \tag{7}$$

and the coherent output power spectrum $W_{s_F s_F}(f)$ is

$$W_{s_F s_F}(f) = \gamma^2_{xy}(f) G_{yy}(f) = G_{s_F s_F}(f) \frac{G_{s_c s_c}(f)}{G_{s_c s_c}(f) + G_{n_1 n_1}(f)} \tag{8}$$

where we assume the extraneous noise terms are uncorrelated with each other and with the signals:

$$G_{s_c n_1}(f) = G_{s_F n_2}(f) = G_{n_1 n_2}(f) = 0 \tag{9}$$

The quantity $W_{s_F s_F}(f)$ can also be called the coherent combustion noise spectrum. Thus, the estimated coherent output power spectrum, $W_{s_F s_F}(f) = \gamma^2_{xy}(f) G_{yy}(f)$, will determine $G_{s_F s_F}(f)$ when the input noise is zero, $G_{n_1 n_1}(f) = 0$, regardless of the output noise $G_{n_2 n_2}(f)$. In the frequency range of interest, we may assume $G_{n_1 n_1}(f) = 0$ or just consider that $W_{s_F s_F}(f)$ is a measure of the coherent combustion noise.

## IV. Sensors, Arena Layout, and Signal Processing

The turbofan engine had a high-temperature pressure sensor with air cooling in a combustor igniter port. An inflow control device was used to prevent turbulent stretched vortex structures from interacting with the fan. The engine condition power settings discussed are 48, 54, and 60% of the maximum power setting. The microphone location used to obtain the results discussed herein is at 130 deg. The signal estimation parameters used are shown in Table 1.

The test was conducted when the air temperature was about 9°C (48°F) and the microphone radius was 30.48 m. The engine was at a height of 3.048 m. Consequently, with a speed of sound of 337 m/s, the travel time for a signal to leave the combustor and reach a microphone is about 90.44 ms (5927 samples). This will be called the measured time delay herein. Using the analysis parameters shown in Table 1, the segment length $T_d = 1/16$ s is 62.5 ms (4096 samples). Consequently, if one calculates the coherence of the combustor pressure transducer signal $K(t)$ and a microphone signal $M(t)$, using the measured time histories, one finds the coherence is that of random noise because the two signals are totally independent except at frequencies where tones are present, as discussed by Miles (2006) [49]. This is due to the fact that the origin of the two signals does not

**Table 1 Spectral estimate parameters**

| Parameter | Value |
|---|---|
| Segment length, i.e., data points per segment, $N$ | 4096 |
| Sample rate $r$, samples/s | 65,536 |
| Segment length, $T_d = N/r$, s | 0.0625 |
| Sampling interval, $\Delta t = 1/r$, s | $1/65,536$ |
| Frequency step, $\Delta f = 1/T_d$, Hz | 16.0 |
| Upper frequency limit, $f_c = 1/2\Delta t = r/2$, Hz | 32,768 |
| Number of frequencies, $Ly = f_c/\Delta f = N/2$ | 2,048 |
| Propagation time delay/lag ($T = 9$°C, $r = 30.48$ m) $D = 5927/65,536$, s | 0.09044 |
| Number of independent samples, $n_s$ | 1120 |
| Overlap | 0.50 |
| Sample length, s | 70 |

overlap in the signal processing interval specified by the segment length $T_d$. The noise coherence confidence threshold interval value is approximately given by (see [49])

$$\gamma_{nn}^2 = \gamma_{KM}^2(f, D > T_d) = 1 - (1 - P)^{1/(n_s - 1)} \tag{10}$$

where this formula determines a $P$-percent threshold confidence interval. Thus the 95% confidence interval noise floor is $\gamma_{nn}^2 = 0.00267$ ($n_s = 1120$).

To align the two signals, the far-field microphone signal can be adjusted by moving it backward using a time delay of $D = 0.09044 \times 65,536 = 5927$ samples based on the signal propagation time. Using computer code, a new aligned array of time history values can be created for each microphone signal. This new array will then be more in phase with the combustor pressure transducer signal. In FORTRAN, the computer code statements that create the new time history are

```
do j = 1, Total_number_of_samples
M_aligned(j) = M_unaligned(j + 5927)
enddo
```

This code slides the points beyond point 5927 backward to align with the $K(t)$ sequence of points, thereby removing the time delay.

This approach does not take into account a multiplicity of reasons why this travel time delay calculated from the speed of sound and microphone radius might not be best. For example, the center of the 100 ft microphone radius might not correspond to the origin of the sound. In addition, no wind gradient or temperature profiles are used, though they might be important in some cases. A discussion on how one can use spherical decay to account for engine noise component source locations is given by Salikuddin et al. (2006) [54].

A slightly more sophisticated procedure to obtain the alignment time $D$ was used herein. The correct time delay minimizes the change of the cross-spectrum phase-angle change with frequency in the range of maximum coherence. Consequently, cross-spectrum phase angles were calculated using correction time delay $D$ values in the range of 1000–9000 in 100 count steps. Because the sample rate $r$ is 65,536 samples/s, the time delay resolution is $100/65,536 = 1.53$ ms. From these cross-spectrum phase-angle plots, the best value of $D$ was selected based on the criterion that the variation of the phase angle with frequency will have a gradient of zero when the time histories are aligned. Again, this value is also the value of $D$ that maximizes the coherence in the frequency range of interest. In some cases, as discussed in [32], when using this procedure, an increase in coherence of 15–27% was noted over the use of a universal $D$ value based on travel time calculated using the measured microphone radius and a speed of sound based on the air temperature.

## V. Phase-Angle Standard Deviation

The coherence function is especially important because the cross-spectrum phase-angle $\theta_{xy}(f)$ standard deviation can be related to the coherence function. In Bendat (1980) [52] and in Piersol (1981) [55], the random error in the phase estimates due to statistical sampling is given in terms of the standard deviation of the estimated phase angle $\bar{\theta}_{xy}(f)$ by

$$\sigma[\bar{\theta}_{xy}(f)] \approx \sin^{-1}\left\{\frac{[1 - \gamma_{xy}^2(f)]^{1/2}}{|\gamma_{xy}|\sqrt{2n_s}}\right\} \tag{11}$$

where $\sigma[\bar{\theta}_{xy}(f)]$ is measured in radians and, as used herein, $n_s$ is selected to be the number of segments or blocks used in the spectral calculations. For the special case in which the term in curly brackets is small, Eq. (11) becomes

$$\sigma[\bar{\theta}(f)] \approx \frac{[1 - \gamma_{xy}^2(f)]^{1/2}}{|\gamma_{xy}|\sqrt{2n_s}} \tag{12}$$

where, for the unknown coherence $\gamma_{xy}^2(f)$, the estimated coherence $\bar{\gamma}_{xy}^2(f)$ is used. A plot of the standard deviation of the phase angle in degrees versus coherence is shown in Fig. 1 for $n_s = 234, 468, 1120$, and 2240. When the coherence is 0.003, Fig. 1 shows the pressure sensor cross-spectrum phase-angle standard deviation should be between 15 and 25 deg. Only phase angles with coherence values greater than 0.003 will be shown in the cross-spectrum phase-angle plots.

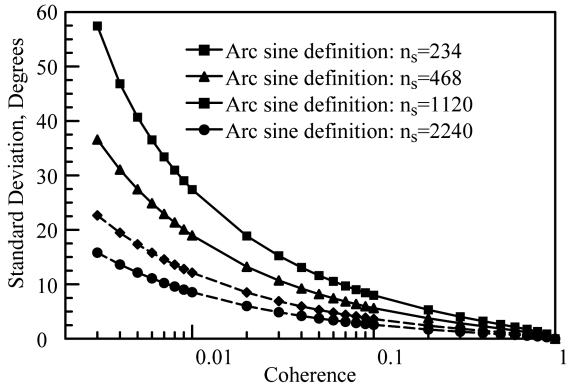


**Fig. 1 Standard deviation of $G_{xy}$ phase angle as a function of $\gamma_{xy}^2$ for $n_s = 234, 468, 1120$, and 2240.**

## VI. Results

Results at the 130 deg microphone are presented in groups arranged by time delay and engine speed. Figures 2–4 present the $D = 90.027$ ms indirect combustion noise source results for the cases at 48, 54, and 60% of the maximum speed. Figures 5–7 present the $D = 86.975$ ms direct combustion noise source results for the cases at 48, 54, and 60% of the maximum speed. Figures 2a, 3a, 4a, 5a, 6a, and 7a show the coherence on a logarithmic scale so that the aligned and unaligned coherence and the statistical noise floor coherence, $\gamma_{nn}^2 = 0.00267$ ($n_s = 1120$), can be clearly revealed as a function of frequency. Figures 2b, 3b, 4b, 5b, 6b, and 7b show the cross-spectrum phase angle as a function of frequency. Figures 2c, 3c, 4c, 5c, 6c, and 7c show the sound pressure level density and the coherent combustion noise spectral density [Eq. (8)] calculated using the aligned and unaligned coherence and the statistical threshold coherence level of two unaligned signals. On each figure, the signal propagation value of $D$ that was used is shown in counts and seconds.

### A. Coherence

For each engine speed case, the aligned and unaligned coherence values are shown in part a of the figure. In addition, the noise floor threshold coherence value of $\gamma_{nn}^2 = 0.00267$ is shown. The coherence is largest in the 0–400 Hz frequency range. The improved coherent output power spectrum method is needed to determine the coherent combustion noise spectrum due to the low coherence levels.

To illustrate the sensitivity of the results to proper selection of the time delay $D$, we note that, to remove the gradient of the phase angle versus frequency in the frequency range from 0 to 200 Hz shown for the 130 deg microphone in Figs. 2–4, for the 48, 54, and 60% of the maximum power setting, the time delay used is $D = 5900/65,536 = 90.027$ ms. However, to remove the gradient of the phase angle versus frequency in the frequency range from 200 to 400 Hz shown for the 130 deg microphone in Figs. 5–7 at the three power settings, the time delay used is $D = 5700/65,536 = 86.975$ ms. This indicates that the noise in the 200–400 Hz frequency band has traveled faster than the noise in the 0–200 frequency band. The actual values of the coherence and the two signal coherent output power spectra do not change much because the signal alignment using either time delay is fine.

Miles et al. (1983) [27] has shown that the acoustic pressure and temperature fluctuations are related and that the cross-spectrum phase angle depends mainly on the slowest propagation speed, which is that of the entropy fluctuation in the flow. Consequently, on the

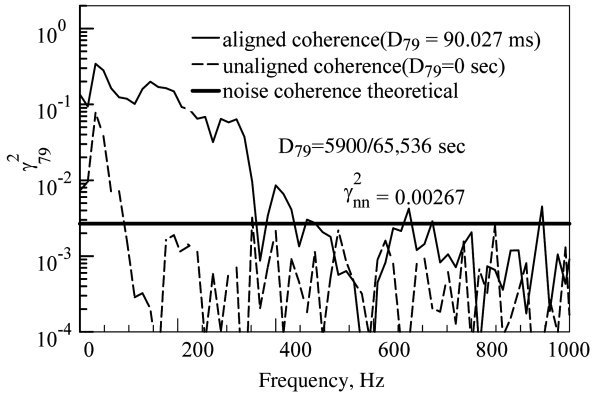


**a) Coherence between microphone at 130 deg and CIP1 combustor pressure sensor**

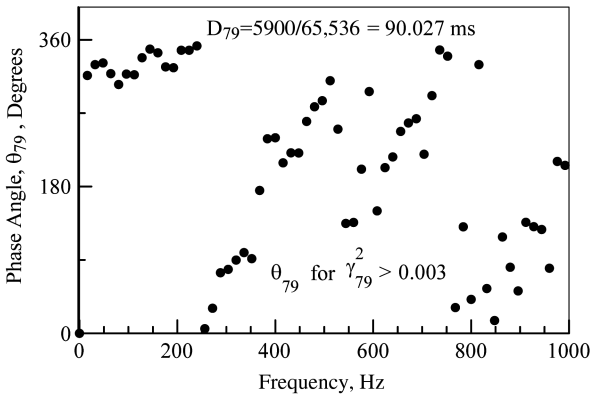


**b) Aligned cross-spectrum phase angle between microphone at 130 deg and CIP1 combustor pressure sensor**

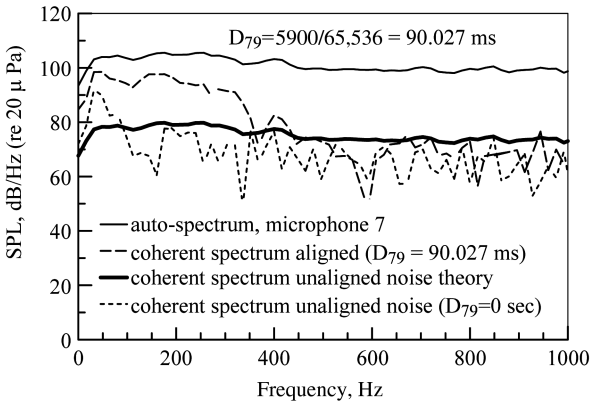


**c) Coherent output power at microphone at 130 deg using CIP1 combustor pressure sensor**

**Fig. 2 Turbofan engine power setting of 48% of maximum power. Microphone at 130 deg ($D_T = 5900/65,536 = 90.027$ ms, indirect combustion noise).**

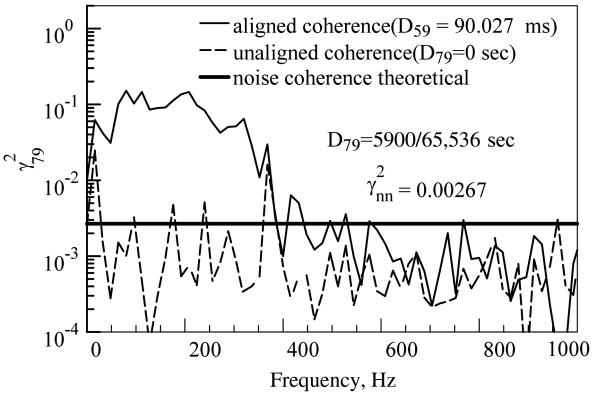


**a) Coherence between microphone at 130 deg and CIP1 combustor pressure sensor**

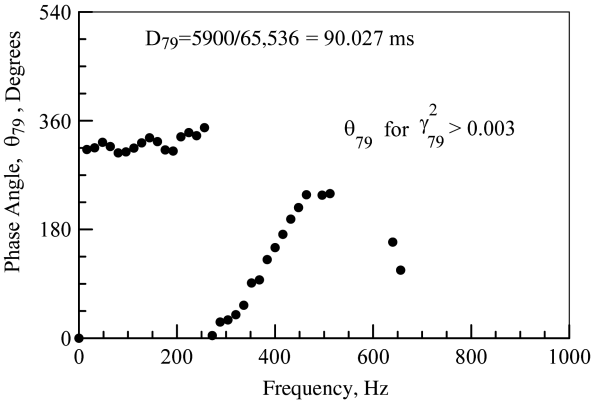


**b) Aligned cross-spectrum phase angle between microphone at 130 deg and CIP1 combustor pressure sensor**

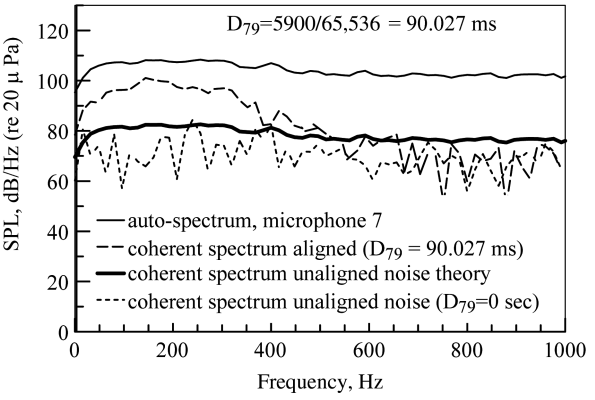


**c) Coherent output power at microphone at 130 deg using CIP1 combustor pressure sensor**

**Fig. 3 Turbofan engine power setting of 54% of maximum power. Microphone at 130 deg ($D_T = 5900/65,536 = 90.027$ ms, indirect combustion noise).**

basis of the time delay ($D = 5900/65,536 = 90.027$ ms) used to remove cross-spectrum phase-angle changes with frequency, we make the argument that, below 200 Hz, the coherence is due mainly to an indirect combustion noise process due to entropy waves, which spend part of the time traveling at the flow velocity (in the combustor). Also, again on the basis of the time delay ($D = 5700/65,536 = 86.975$ ms) used to remove cross-spectrum phase-angle changes with frequency in the 200–400 Hz band, this coherence is due mainly to a direct combustion noise source, which spends all its time propagating as an acoustic wave.

Similar behavior was identified for all three power settings at the 110 deg microphone where the indirect (entropy) noise signal time was 93.079 ms and the direct (acoustic) noise signal travel time was 90.027 ms. Furthermore, similar behavior was also identified for all three power settings at the 160 deg microphone where the indirect (entropy) noise signal time was 84.449 ms and the direct (acoustic) noise signal travel time was 82.397 ms. The difference is a consistent 200 counts or 3.052 ms for all the aft-quadrant polar directivity angles. However, note that the time-step interval used in this study was 100 counts or 1.53 ms. Consequently, this is one item future experiments could improve upon.

It is likely that the measured coherence represents, in reality, a combination of direct and indirect noise sources and that some time delay, which is a function of frequency, should be used to remove the cross-spectrum phase-angle changes. However, that investigation is beyond the scope of this report. Because the time delays are the result

of a combination of sources without a detailed source acoustic and propagation model, detailed geometry and detailed performance information, it is difficult to assign precise velocities and lengths to obtain these time delay values.

Muthukrishnan et al. (1978) [26] make a similar argument that, at low frequencies, a high coherence exists between combustion noise and entropy noise. However, they argue that, at moderate frequencies, the phase becomes rapidly oscillatory which destroys the coherence and makes the entropy noise and combustion noise independent, uncorrelated sources. Consequently, the combustor pressure at low frequencies is coherent with entropy noise. At higher frequencies, it is coherent with direct combustion noise.

In any event, the cross spectra between the combustion sensor pressure signal and the far-field microphone pressure signal provides some indication that the time delay before the indirect mechanism changes an entropy fluctuation into an acoustic wave can be estimated, and direct and indirect coherent combustion noise can be separated.

### B. Tones in the Coherence

As discussed by Miles (2006) [49], tones can be identified using the aligned and unaligned coherence function. The unaligned coherence function has a value determined by the number of samples of two independent signals and the tones. The aligned signal has a value determined by the coherence of the two signals and tones. For the engine condition power setting of 48%, a strong tone occurs at 352 Hz. For the engine condition power setting of 54%, a strong tone

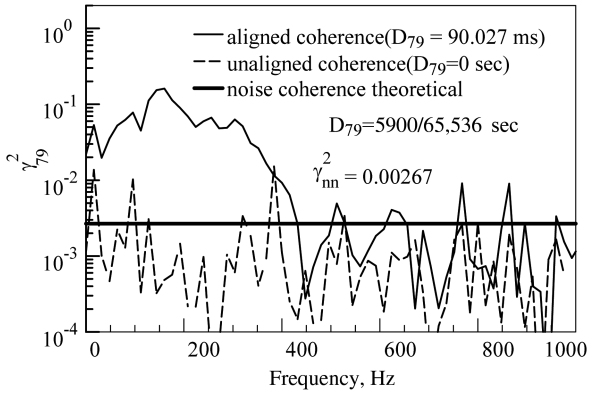


**a) Coherence between microphone at 130 deg and CIP1 combustor pressure sensor**

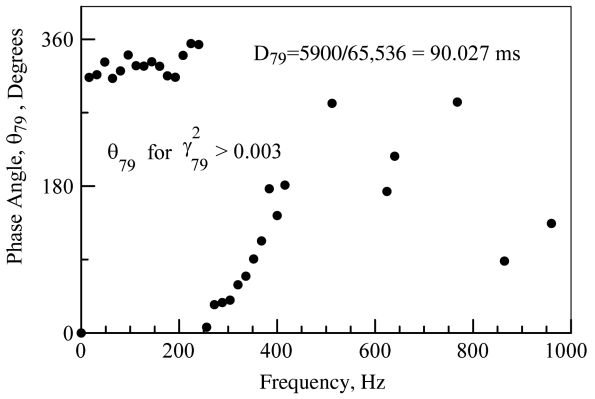


**b) Aligned cross-spectrum phase angle between microphone at 130 deg and CIP1 combustor pressure sensor**

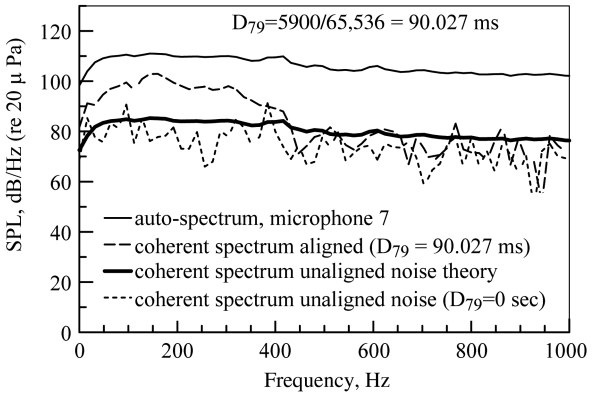


**c) Coherent output power at microphone at 130 deg using CIP1 combustor pressure sensor**

**Fig. 4 Turbofan engine power setting of 60% of maximum power. Microphone at 130 deg. ($D_T = 5900/65,536 = 90.027$ ms, indirect combustion noise).**

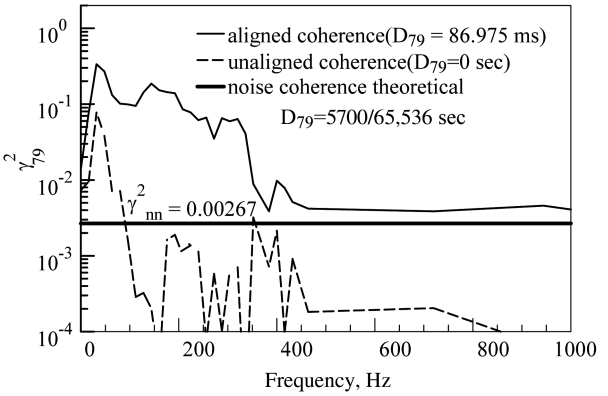


**a) Coherence between microphone at 130 deg and CIP1 combustor pressure sensor**

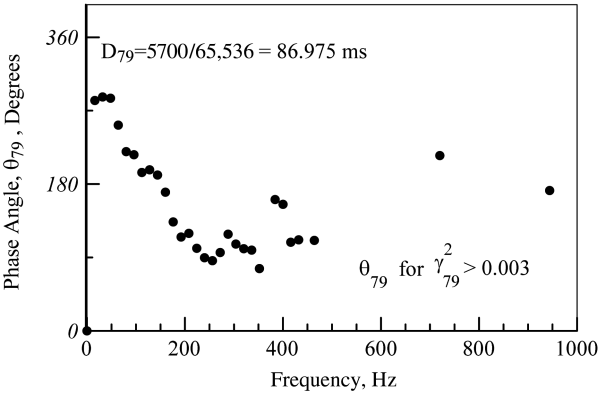


**b) Aligned cross-spectrum phase angle between microphone at 130 deg and CIP1 combustor pressure sensor**

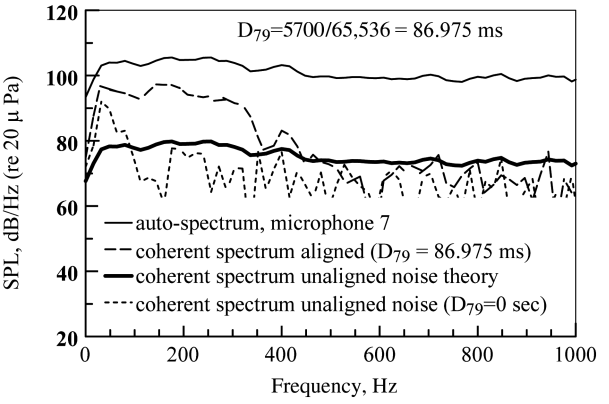


**c) Coherent output power at microphone at 130 deg using CIP1 combustor pressure sensor**

**Fig. 5 Turbofan engine power setting of 48% of maximum power. Microphone at 130 deg ($D_T = 5700/65,536 = 86.975$ ms, direct combustion noise).**

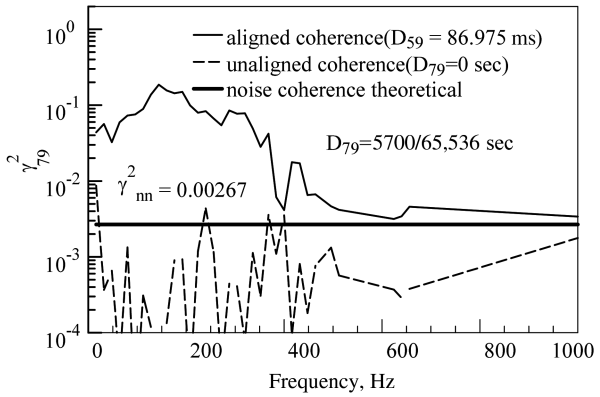


**a) Coherence between microphone at 130 deg and CIP1 combustor pressure sensor**

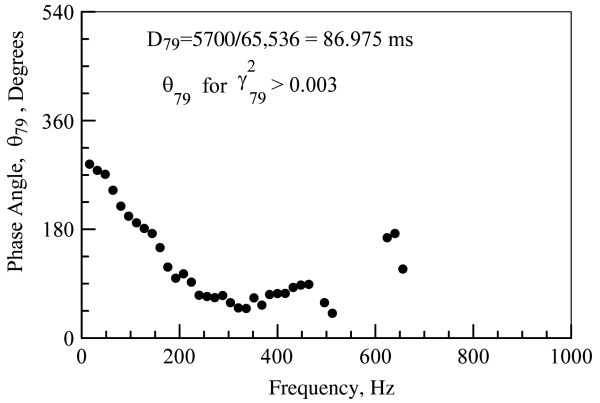


**b) Aligned cross-spectrum phase angle between microphone at 130 deg and CIP1 combustor pressure sensor**

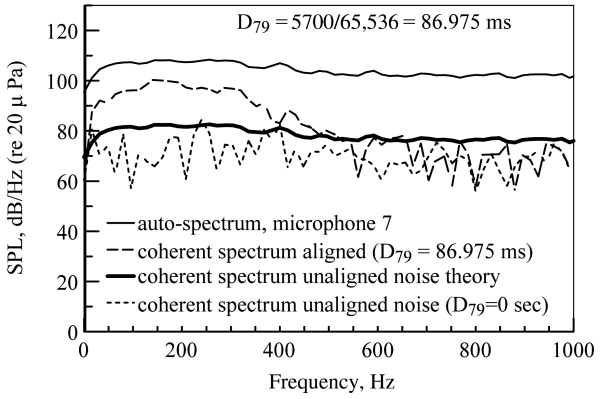


**c) Coherent output power at microphone at 130 deg using CIP1 combustor pressure sensor**

**Fig. 6 Turbofan engine power setting of 54% of maximum power. Microphone at 130 deg ($D_T = 5700/65,536 = 86.975$ ms, direct combustion noise).**

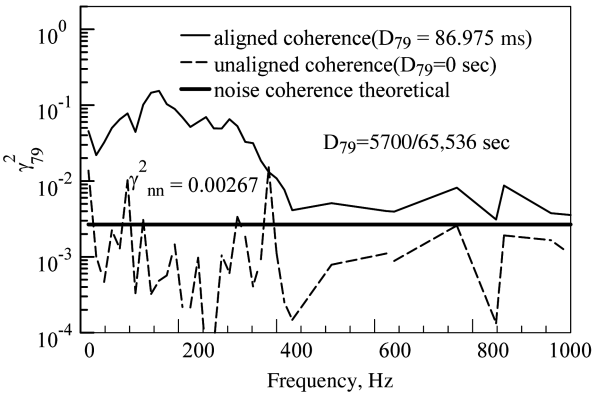


**a) Coherence between microphone at 130 deg and CIP1 combustor pressure sensor**

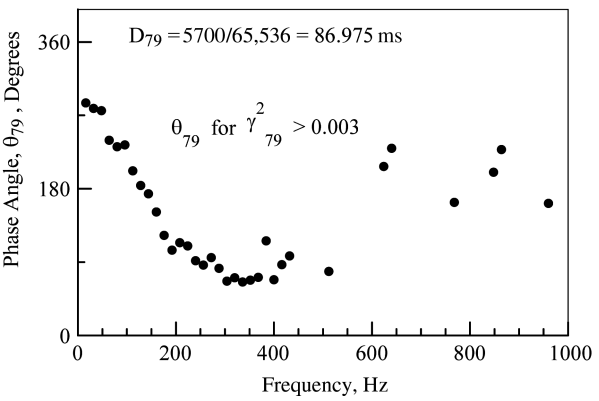


**b) Aligned cross-spectrum phase angle between microphone at 130 deg and CIP1 combustor pressure sensor**

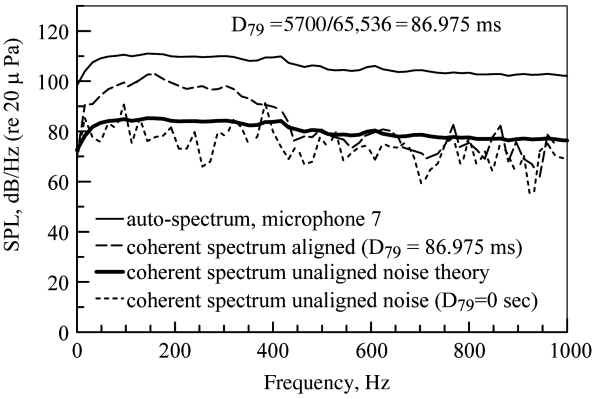


**c) Coherent output power at microphone at 130 deg using CIP1 combustor pressure sensor**

**Fig. 7 Turbofan engine power setting of 60% of maximum power. Microphone at 130 deg ($D_T = 5700/65,536 = 86.975$ ms, direct combustion noise).**

occurs at 368 Hz. For the engine condition power setting of 60%, a strong tone occurs at 384 Hz.

These tones can be related to the shaft frequency of the N2 concentric shaft, which connects the high-pressure compressor and the high-pressure turbine spool (see Sec. II). The shaft frequency is the shaft rotation speed in revolutions per minute divided by 60 to convert the value into cycles per second or hertz. The physical N2 shaft rotation rates are 21,340; 22,310; and 22,930 rpm, which correspond to shaft frequencies of 355.667, 371.83, and 382 Hz. Because the bandwidth being used is 16 Hz, the observed tones correspond to the physical N2 shaft frequency. Consequently, these tones appear to be compressor tones possibly related to a compressor disk tone.

### C. Cross-Spectrum Phase Angle

If the coherence is larger than 0.003, the phase-angle standard deviation with $n_s > 2000$ is between 15 and 25 deg (see Fig. 1). Consequently, the phase-angle plots emphasize measured phase angles where the coherence is greater than 0.003.

## VII. Discussion

The correlated far-field core noise component from the turbofan engine covers the frequency range from 0 to 400 Hz. Coherence function results showing correlated core noise in the frequency range from 0 to 400 Hz were obtained by Miles (2006) [49] in the study of a Pratt and Whitney PW4098 turbofan engine, by Siller et al. (2001)

**Table 2 Some engine specifications**

| Engine | Number of fuel nozzles | Nominal bypass ratio | Typical max. combustor/core to far-field coherence $\gamma^2$ at 120–160 deg |
|---|---|---|---|
| AVCO Lycoming YF102 [39] | 28 | 6:1 | 0.5 |
| General Electric CF6-50 [44] | 30 | 4.4:1 (takeoff) | 0.1 |
| Pratt and Whitney JT15D [45] | 12 | 3.3:1 | 0.5 |
| Pratt and Whitney JT9D [46] | 20 | 5:1 | 0.4 |
| Pratt and Whitney PW4098 [49] | 24 | 5.8 | 0.1 |
| Honeywell TECH977 (HTF7000) | 16 | 4.2 | 0.35 |

[48] in the study of core noise from a Rolls-Royce BR700 aeroengine, and in the study of an AVCO Lycoming YF-102 by Karchmer and Reshotko (1976) [39], and Karchmer (1977) [40].

Karchmer (1983) [56] in the study of AVCO Lycoming YF-102 core noise, and Miles (2006) [49] in the study of core noise from a Pratt and Whitney PW4098, attribute this coherent noise to the lowest radial order modes of the combustion noise. The lowest radial order mode is the $m = 0$ mode, which corresponds to a plane wave. Karchmer (1983) [56] used six pressure probes to identify combustor modes. Miles (2007) [57] used a restricted acoustic model analysis using signals from two combustor pressure sensors to identify combustor modes.

The turbofan combustor is designed to have a high level of turbulence without being unstable. As far back as 1957, Blackshear and Rayle (1957) [58] mention that some observers report beneficial effects due to velocity and pressure excursions evidenced in a noticeable increase in the combustion efficiency within the combustor. Poinsot and Veynante (2005) [59] (see p. 131) remark that the main effect of turbulence on combustion is to increase the combustion rate. Hill and Peterson (1992) [60] mention that more intense turbulence promotes more rapid mixing of the vaporized fuel and air and faster propagation of flame through the unburned mixture. They present a good discussion of gas turbine combustor fundamental design issues.

The coherence measurements in turbofan engines between the combustor and the far-field microphones differ from those made using a combustor burner assembly with a single fuel spray nozzle, as used by Strahle et al. (1977) [25] and Muthukrishnan et al. (1978) [47], due to the presence of the fan inlet sound source, the fan exhaust sound source, the jet sound source, the turbine self-noise source, and the combustor–turbine interaction. The coherence measurements in turbofan engines are influenced by the fact that turbofan engines have an annular combustor which allows circumferential modes. In addition, the coherence measurements should reflect the possibility of entropy noise from hot spots passing through the turbine, as discussed by Pickett (1975) [12], Cumpsty and Marble (1977) [13], and Gliebe et al. (2000) [16], as well as direct combustion noise and compressor tones. However, coherence measurements made using a combustor burner assembly with a single fuel spray nozzle, as used by Strahle et al. (1977) [25] and Muthukrishnan et al. (1978) [47], do have a jet noise source and the possibility of entropy noise from hot spots passing through an exit nozzle, as described by Williams and Howe (1975) [19] and Marble and Candel (1977) [20].

Table 2 shows that, for a great number of combustion chamber geometries, range of the number of nozzles, and engine design bypass ratios, significant coherence can be measured from 120 to 160 deg. The combustion duct modal analysis of Karchmer (1983) [56] and Miles (2007) [57] suggest that the coherence is due to annular combustion duct modes propagating to the far field, and, at the lowest frequencies, the coherence is from a plane wave combustion duct mode. The interesting aspect is that one sees any coherence at all considering each fuel nozzle is an independent source of noise and the level of turbulence used to increase combustor efficiency and reduce emissions is high.

For many engines, the coherence in the far field is less than 0.1 and one may use the method of aligned and unaligned coherence developed by Miles (2006) [49] to determine if the coherence is significant. Note, for example, that, for the CF6-50 core noise investigation described by Doyle and Moore (1980) [44], the number of samples was 100, and the 95% threshold coherence level for two independent signals using 100 samples is $\gamma^2_{nn} = 1 - (1 - 0.95)^{1/(100-1)} = 0.0298$. Doyle and Moore (1980) [44] plotted coherence values on a linear scale from 0 to 1.0, and coherence values less than 0.1 were ignored. To some extent, the coherence value of 0.1 has traditionally been considered a threshold or "cutoff" level of coherence. The discussion presented herein shows that this is not a realistic value for modern turbofan engines.

The sound radiation spectrum of flames is a topic of current experimental research by Rajaram et al. (2004, 2006) [9,61] and computational fluid dynamic research using the large-eddy simulation technique by Ihme et al. (2006) [10]. In addition, research to study the interaction of sound and flames is being conducted by Lieuwen and Cho (2005) [62], and the effect of noise on combustion stability is being studied by Lieuwen and Banaszuk (2005) [63]. However, there is a gap between these studies of the acoustics of a flame from a fuel spray nozzle and the acoustical interaction of multiple fuel spray combustor nozzles in an annular combustor. The mechanism leading to the formulation of annular acoustic duct modes from the sound generated by multiple independent fuel spray nozzles is unknown. The amount of the total sound energy participating in the annular duct modes is unknown. If only part of the total sound energy is measured by the coherence function from the combustor to the far field, then the remainder will show up in the far field as radiated sound unattributable to the combustor noise. Perhaps the annular acoustic duct modes represent a steady-state phenomena as sound energy is added by the multiple spray combustor nozzles and removed as sound leaves the combustor. At the moment, the ratio of uncorrelated sound to coherent sound in the combustor duct is an open question.

Several core noise prediction procedures based on direct combustion noise are available that use a single spectral segment with a peak in the 400–500 Hz frequency band [23,64–68]. The SAE 876 (1978) [68] method is based on the results discussed by Emmerling et al. (1976) [66], and this procedure is used in the 1982 and current Aircraft Noise Prediction Program (ANOPP) [69]. Validation studies of the ANOPP code reported by Shivashankara (1980) [70] showed predictions in good agreement with flyover data at an aft microphone position of 120 deg in the frequency range from 400 to 630 Hz. Validation studies of the ANOPP code by Kontos et al. (1996) [71] showed that the core noise predictions did no harm in creating unreasonable spectral shapes or levels that exceeded the level of the total measured engine noise. The results presented herein show the peak core combustion noise is at a frequency less than 400 Hz. The results discussed herein show that both indirect and direct combustion noise sources are present. A core noise prediction procedure based on using more than one spectral segment was proposed by von Glahn and Krejsa (1982) [72]. This type of procedure could account for both indirect and direct combustion noise sources, which is not being done currently and might produce a better prediction.

## VIII. Conclusions

The source location technique based on adjusting the time delay between the combustor pressure sensor signal and the far-field microphone signal to maximize the coherence and remove as much variation of the phase angle with frequency as possible was successful in identifying frequency bands dominated by direct and indirect combustion noise. A method to help identify combustion noise coherence using an aligned and unaligned coherence

technique, which enables the validation of low levels of coherence as being due to core noise by identifying the coherence noise floor, has been demonstrated. A statistical procedure was also used to establish this threshold level.

Using the procedures discussed led to the discovery that, for this particular engine, the turbofan core noise in the 200–400 Hz frequency band is chiefly related to coherent direct combustion noise, which travels from the combustor to the far field as an acoustic signal. Furthermore, it was found that the noise signal in the 0–200 Hz frequency band is chiefly related to coherent indirect combustion noise due to entropy fluctuations, which travel at the flow velocity in the combustor and turbine until an interaction with turbine-stage pressure gradients converts these entropy fluctuations into acoustic waves.

## Acknowledgment

The acoustic time histories analyzed herein were made available by Honeywell Aerospace as part of the NASA/Honeywell Engine Validation of Noise and Emissions Reduction Technology program under provisions of NASA Contract NAS3-01136 from tests conducted by Honeywell Aerospace at the San Tan test site located southeast of Phoenix, Arizona.

## References

[1] Chu, B.-T., "Pressure Waves Generated by Addition of Heat in a Gaseous Medium," NACA, TR NACA TN 3411, 1955.

[2] Strahle, W. C., "On Combustion Generated Noise," *Journal of Fluid Mechanics*, Vol. 49, 1971, pp. 399–414. doi:10.1017/S0022112071002167

[3] Lighthill, M. J., "On Sound Generated Aerodynamically, I: General Theory," *Proceedings of the Royal Society of London, Series A: Mathematical and Physical Sciences*, Vol. 211, No. 11071952, pp. 564–587. doi:10.1098/rspa.1952.0060

[4] Lighthill, M. J., "On Sound Generated Aerodynamically, II: Turbulence as a Source of Sound," *Proceedings of the Royal Society of London, Series A: Mathematical and Physical Sciences*, Vol. 222, No. 1148Feb. 1954, pp. 1–32. doi:10.1098/rspa.1954.0049

[5] Strahle, W. C., "Some Results in Combustion Generated Noise," *Journal of Sound and Vibration*, Vol. 23, No. 1, 1972, pp. 113–125. doi:10.1016/0022-460X(72)90792-4

[6] Strahle, W. C., and Shivashankara, B. N., "A Rational Correlation of Combustion Noise Results from Open Turbulent Premixed Flames," *Fifteenth Symposium (International) on Combustion*, Combustion Inst., Pittsburgh, PA, 1975, pp. 1379–1385.

[7] Strahle, W. C., "The Convergence of Theory and Experiment in Direct Combustion Generated Noise," AIAA 1975-522, March 1975, NASA Grant NSG-3015; AF-AFOSR-72-2385.

[8] Rajaram, R., and Lieuwen, T., "Parametric Studies of Acoustic Radiation from Premixed Flames," *Combustion Science and Technology*, Vol. 175, No. 12, Dec. 2003, pp. 2269–2298. doi:10.1080/714923281

[9] Rajaram, R., Gray, J., and Lieuwen, T., "Premixed Combustion Noise Scaling: Total Power and Spectra," AIAA Paper 2006-2612, May 2006.

[10] Ihme, M., Bodony, D. J., and Pitsch, H., "Prediction of Combustion-Generated Noise in Non-Premixed Turbulent Jet Flames Using Large-Eddy Simulation," AIAA Paper 2006-2614, May 2006.

[11] Dowling, A. P., "Thermoacoustic Sources and Instabilities," *Modern Methods in Analytical Acoustics: Lecture Notes*, edited by D. G. Crighton, A. P. Dowling, J. F. Williams, M. Heckel, and F. Leppington, Springer–Verlag, New York, 1992, Chap. 13, pp. 378–403.

[12] Pickett, G. F., "Core Engine Noise Due to Temperature Fluctuating Through Turbine Blade Rows," AIAA Paper 75-528, 1975.

[13] Cumpsty, N. A., and Marble, F. E., "The Interaction of Entropy Fluctuations with Turbine Blade Rows: A Mechanism of Turbojet Noise," *Proceedings of the Royal Society of London, Series A: Mathematical and Physical Sciences*, Vol. 357, No. 16901977, pp. 323–344. doi:10.1098/rspa.1977.0171

[14] Cumpsty, N. A., and Marble, F., "Core Noise from Gas Turbine Exhausts," *Journal of Sound and Vibration*, Vol. 54, No. 2, 1977, pp. 297–309. doi:10.1016/0022-460X(77)90031-1

[15] Cumpsty, N. A., "Jet Engine Combustion Noise: Pressure, Entropy and Vorticity Perturbations Produced by Unsteady Combustion or Heat Addition," *Journal of Sound and Vibration*, Vol. 66, No. 4, 1979, pp. 527–544. doi:10.1016/0022-460X(79)90697-7

[16] Gliebe, P., Mani, R., Shin, H., Mitchell, B., Ashford, G., Salamah, S., and Connell, S., "Acoustic Prediction Codes," General Electric Aircraft Engines, TR NASA CR-2000-210244, R99AEB169, Aug. 2000.

[17] Cuadra, E., "Acoustic Wave Generation by Entropy Discontinuities Flowing past an Area Change," *Journal of the Acoustical Society of America*, Vol. 42, No. 4, 1967, pp. 725–732. doi:10.1121/1.1910643

[18] Goldstein, M. E., "Turbulence Generated by the Interaction of Entropy Fluctuations with Non-Uniform Mean Flows," *Journal of Fluid Mechanics*, Vol. 93, No. 2, 1979, pp. 209–224. doi:10.1017/S0022112079001853

[19] Williams, J. E. F., and Howe, M. S., "The Generation of Sound by Density Inhomogeneities in Low Mach Number Nozzle Flows," *Journal of Fluid Mechanics*, Vol. 70, No. 3, 1975, pp. 605–622. doi:10.1017/S0022112075002224

[20] Marble, F. E., and Candel, S. M., "Acoustic Disturbance from Gas Non-Uniformities Convected Through a Nozzle," *Journal of Sound and Vibration*, Vol. 55, No. 2, 1977, pp. 225–243. doi:10.1016/0022-460X(77)90596-X

[21] Strahle, W. C., "Combustion Noise," NASA, TR NASA-CR-162571, 1977.

[22] Strahle, W. C., "Combustion Noise," *Progress in Energy and Combustion Science*, Vol. 4, No. 3, 1978, pp. 157–176. doi:10.1016/0360-1285(78)90002-3

[23] Mathews, D. C., Rekos, N. F., Jr., and Nagel, R. T., "Combustion Noise Investigation," Dept. of Transportation/Federal Aviation Admininstration, TR FAA RD-77-3, Feb. 1977, 77N27873, AS Number: AD038154/1 Class: U, p. 202.

[24] Mathews, D., and Rekos, N. F., Jr., "Prediction and Measurement of Direct Combustion Noise in Turbo-Propulsion Systems," *Journal of Aircraft*, Vol. 14, No. 9, Sept. 1977, pp. 850–859. doi:10.2514/3.58865

[25] Strahle, W. C., Muthukrishnan, M., and Neale, D. H., "Coherence Between Internal and External Noise Generated by a Gas Turbine Combustor," *AIAA Journal*, Vol. 15, No. 7, 1977, pp. 1018–1024. doi:10.2514/3.60744

[26] Muthukrishnan, M., Strahle, W. C., and Neale, D. H., "Separation of Hydrodynamic, Entropy, and Combustion Noise in a Gas Turbine Combustor," *AIAA Journal*, Vol. 16, No. 4, April 1978, pp. 320–327. doi:10.2514/3.60895.

[27] Miles, J. H., Wasserbauer, C. A., and Krejsa, E. A., "Cross Spectra Between Temperature and Pressure in a Constant Area Duct Downstream of a Combustor," AIAA 83-0762, NASA TM-83351, 1983.

[28] Schemel, C., Thiele, F., Bake, F., Lehmann, B., and Michel, U., "Sound Generation in the Outlet Section of Gas Turbine Combustion Chambers," AIAA Paper 2004-2929, 2004.

[29] Richter, C., Panek, L., and Thiele, F. H., "On the Application of CAA-Methods for the Simulation of Indirect Combustion Noise," AIAA Paper 2005-2919, May 2005.

[30] Bake, F., Michel, U., Rohle, I., Richter, C., Thiele, F., Liu, M., and Noll, B., "Indirect Combustion Noise Generation in Gas Turbines," AIAA Paper 2005-2830, May 2005.

[31] Bake, F., Michel, U., and Roehle, I., "Investigation of Entropy Noise in Aero-Engine Combustors," *Journal of Engineering for Gas Turbines and Power*, Vol. 129, April 2007, pp. 370–376. doi:10.1115/1.2364193

[32] Miles, J. H., "Spectral Separation of the Turbofan Engine Coherent Combustion Noise Component," AIAA Paper 2008-50, Jan. 2008; NASA TM-2008-215157, 2008.

[33] Alonso, J., Kwan, H., and Burdisso, R., "EVNERT Program: Testing of Adaptive HQ-Liner for Aft Noise Control," AIAA Paper 2008-2811, May 2008.

[34] Mendoza, J. M., Nance, D. K., and Ahuja, K. K., "Source Separation from Multiple Microphone Measurements in the Far Field of a Full Scale Aero Engine," AIAA 2008-2809, 2008.

[35] Weir, D. S., and Mendoza, J. M., "Baseline Noise Measurements from the Engine Validation of Noise and Emissions Reduction Technology Program," AIAA 2008-2807, 2008.

[36] Schuster, B., "Statistical Considerations for Gas Turbine Engine Noise Measurements," AIAA 2008-2808, 2008.

[37] Royalty, C. M., and Schuster, B., "Noise from a Turbofan Engine Without a Fan from the Engine Validation of Noise and Emission Reduction Technology (EVNERT) Program," AIAA 2008-2810, 2008.

[38] Dougherty, R. P., and Mendoza, J. M., "Nacelle In-Duct Beamforming Using Modal Steering Vectors," AIAA 2008-2812, 2008.
[39] Karchmer, A. M., and Reshotko, M., "Core Noise Source Diagnostics on a Turbofan Engine Using Correlation and Coherence Techniques," NASA TR NASA TMX-73535, 1976.
[40] Karchmer, A. M., "Identification and Measurement of Combustion Noise from a Turbofan Engine Using Correlation and Coherence Techniques," NASA TR NASA TM-73747, 1977; Ph.D. Thesis, Dept. of Mechanical and Aerospace Engineering, Case Western Reserve Univ., Cleveland, OH; NASA Glenn Research Center Performing Organization Rept. No. E-9319.
[41] Reshotko, M., Karchmer, A., Penko, P. F., and McArdle, J. G., "Core Noise Measurements on a YF-102 Turbofan Engine," *Journal of Aircraft*, Vol. 14, No. 7, July 1977, pp. 611–612. doi:10.2514/3.58830
[42] Krejsa, E. A., "Combustion Noise from Gas Turbine Aircraft Engines Measurement of Far-Field Levels," NASA TR TM-88971, 1987.
[43] Shivashankara, B. N., "Gas Turbine Core Noise Source Isolation by Internal-to-Far-Field Correlations," *Journal of Aircraft*, Vol. 15, No. 9, Sept. 1978, pp. 597–600. doi:10.2514/3.58412
[44] Doyle, V. L., and Moore, M. T., "Core Noise Investigation of the CF6-50 Turbofan Engine," General Electric Co. TR R79AEG395, NASA CR-159598, Jan. 1980.
[45] Reshotko, M., and Karchmer, A., "Core Noise Measurements from a Small, General Aviation Turbofan Engine," NASA TR TM-81610, N81-11769, 1980.
[46] Shivashankara, B. N., "High Bypass Ratio Engine Noise Component Separation by Coherence Technique," *Journal of Aircraft*, Vol. 20, No. 3, March 1983, pp. 236–242. doi:10.2514/3.44858; also *7th Aeroacoustics Conference*, AIAA Paper 81-2054, 1981.
[47] Muthukrishnan, M., Strahle, W. C., and Neale, D. H., "Separation of Hydrodynamic, Entropy, and Combustion Noise in a Gas Turbine Combustor," *AIAA Journal*, Vol. 16, No. 4, April 1978, pp. 320–327. doi:10.2514/3.60895
[48] Siller, H. A., Arnold, F., and Michel, U., "Investigation of Aero-Engine Core-Noise Using a Phased Microphone Array," *AIAA/CEAS Aeroacoustics Conference*, AIAA 2001-2269, 2001.
[49] Miles, J. H., "Aligned and Unaligned Coherence: A New Diagnostic Tool," *44th AIAA Aerospace Science Meeting*, AIAA, 2006-0010, 2006; also NASA TM-2006-214112.
[50] Bendat, J. S., and Piersol, A. G., *Measurement and Analysis of Random Data*, Wiley, New York, 1966.
[51] Bendat, J. S., and Piersol, A. G., *Random Data: Analysis and Measurement Procedures*, Wiley, New York, 1971.
[52] Bendat, J. S., and Piersol, A. G., *Engineering Applications of Correlation and Spectral Analysis*, Wiley, New York, 1980.
[53] Karchmer, A., Reshotko, M., and Montegani, F., "Measurement of Far Field Combustion Noise from a Turbofan Engine Using Coherence Functions," AIAA Paper 77-1277, 1977; also NASA TM-73748, N77-33163.
[54] Salikuddin, M., Stimpert, D., and Majjigi, R., "A Method to Account for Engine Noise Component Source Locations," *12th AIAA/CEAS Aeroacoustics Conference; 27th AIAA Aeroacoustics Conference*, AIAA Paper 2006-2554, 2006.
[55] Piersol, A., "Time Delay Estimation Using Phase Data," *IEEE Transactions on Acoustics, Speech, and Signal Processing*, Vol. 29, No. 3, June 1981, pp. 471–477. doi:10.1109/TASSP.1981.1163555
[56] Karchmer, A. M., "Acoustic Modal Analysis of a Full Scale Annular Combustor," AIAA Paper 83-0760, 1983; also NASA TM-83334.
[57] Miles, J. H., "Restricted Modal Analysis Applied to Internal Annular Combustor Auto-Spectra and Cross-Spectra Measurements," *AIAA Journal*, Vol. 45, No. 5, May 2007, pp. 988–999. doi:10.2514/1.25179
[58] Blackshear, P. L., and Rayle, W. D., "Oscillations in Combustors," *Basic Considerations in the Combustion of Hydrocarbon Fuels with Air*, edited by H. C. Barnett and R. R. Hibbard, NACA, TR-1300 VIII, 1957, pp. 229–241.
[59] Poinsot, T., and Veynante, D., *Theoretical and Numerical Combustion*, R. T. Edwards, Philadelphia, 2005.
[60] Hill, P. G., and Peterson, C. R., *Mechanics and Thermodynamics of Propulsion*, Addison Wesley, Reading, MA, 1992.
[61] Rajaram, R., and Lieuwen, T., "Effect of Approach Flow Turbulence Characteristics on Sound Generation from Premixed Flames," *42nd AIAA Aerospace Sciences Meeting and Exhibit*, AIAA Paper 2004-461, 2004.
[62] Lieuwen, T., and Cho, J. H., "Coherent Acoustic Wave Amplification/Damping by Wrinkled Flames," *Journal of Sound and Vibration*, Vol. 279, Nos. 3–5, 2005, pp. 669–686. doi:10.1016/j.jsv.2003.11.050
[63] Lieuwen, T., and Banaszuk, A., "Background Noise Effects on Combustor Stability," *Journal of Propulsion and Power*, Vol. 21, No. 1, Jan.–Feb. 2005, pp. 25–31. doi:10.2514/1.5549
[64] Dunn, D. G., and Peart, N. A., "Aircraft Noise Source and Contour Estimation," NASA TR CR-114649, 1973.
[65] Huff, R. G., Clark, B. J., and Dorsch, R. G., "Interim Prediction Method for Low Frequency Core Engine Noise," NASA Glenn Research Center, TR NASA TM X-71627, 1974.
[66] Emmerling, J. J., Kazin, S. B., and Matta, R. K., "Core Engine Noise Control Program Volume III, Supplement I: Prediction Methods," General Electric, TR FAA-RD-74-125,III-I, AD A030376, 1976.
[67] Mathews, D. C., and Rekos, N. F., Jr., "Prediction and Measurement of Direct Combustion Noise in Turbopropulsion Systems," *Journal of Aircraft*, Vol. 14, No. 9, Sept. 1977, pp. 850–859. doi:10.2514/3.58865
[68] Anon., "Gas Turbine Jet Exhaust Noise Prediction," Society of Automotive Engineers, TR ARP876, 1978.
[69] Zorumski, W. E., "Aircraft Noise Prediction Program Theoretical Manual, Part 1 and Part 2," NASA, TR NASA-TM-83199 Pt. 1 and Pt. 2, 1982.
[70] Shivashankara, B. N., "Aircraft Noise Prediction Program Validation," NASA, TR NASA CR-159333, 1980.
[71] Kontos, K. B., Janardan, B. A., and Gliebe, P. R., "Improved NASA-ANOPP Noise Prediction Computer Code for Advanced Subsonic Propulsion Systems, Volume 1: ANOPP Evaluation and Fan Noise Model Improvement," NASA, TR CR 195480, 1996.
[72] von Glahn, U., and Krejsa, E., "Correlation of Core Noise Obtained by Three-Signal Coherence Techniques," NASA Lewis Research Center, TR NASA TM83012, 1982.

K. Frendi
*Associate Editor*